Aminoacyl−Anthraquinone Conjugates as Telomerase Inhibitors: Synthesis, Biophysical and Biological Evaluation

Giuseppe Zagotto,[†] Claudia Sissi,[†] Lorena Lucatello,[†] Claudia Pivetta,[†] Sergio A. Cadamuro,[†] Keith R. Fox,[‡] Stephen Neidle,[§] and Manlio Palumbo*,[†]

Department of Pharmaceutical Sciences, University of Padova, Via Marzolo 5, 35131 Padova, Italy, School of Biological Sciences, University of Southampton, Bassett Crescent East, Southampton SO16 7PX, United Kingdom, CRUK Biomolecular Structure Group, The School of Pharmacy, University of London, London WC1N 1AX, United Kingdom

Received February 15, 2008

The telomerase−telomere complex is a prospective anticancer target. To inhibit enzyme activity by induction of G-quadruplex in human telomeres, we have synthesized a small library of 2,6- and 2,7-amino-acyl/peptidyl anthraquinones with diverse connecting linkers, charge, lipophilicity and bulk. The test compounds modulated G-quadruplex stability to different extents and showed clear preference for quadruplex over duplex DNA. Telomerase inhibition correlated with G-quadruplex stabilization. A SAR analysis showed that type of linkage between the linker and the anthraquinone, together with the position of the side chains and the nature of the amino acid components play a major role both in stabilizing G-quadruplex and producing telomerase inhibition. Short-term cytotoxic activity was poor. However, after prolonged exposure to effective G-quadruplex binders, cells became senescent. These results are of help in the rational design of more efficient G-quadruplex stabilizers, possibly endowed with cancer cell-selective antiproliferative effects.

Introduction

Single-stranded nucleic acids, depending upon their sequences, can fold into several secondary structure types. Although genomic DNA is mainly present along with its complementary strand in a double-helical arrangement, many sequences can form intramolecular structures under physiological conditions.[1] In particular, guanine-rich DNA and RNA sequences can assume G-quadruplex structures.[2] They are based on stacks of square-planar arrays of G-tetrads, consisting of four guanines that are linked together by Hoogsteen-type base pairing. Monovalent cations (in particular potassium ions) can stabilize these structures through coordination with the eight carbonyl groups facing the central cavity defined by the G-tetrads. G-quadruplexes can be formed by the intramolecular folding of one strand containing at least four G-rich tracts or by the intermolecular association of a variable number of DNA strands. Additionally, these structures are highly polymorphic with respect to several mutually related factors: orientation of the strands, *syn*/*anti* glycosidic bond conformation, loop connectivities, and sequence.[3]

Particular attention has recently been paid to the G-rich sequences that form telomeres, the noncoding regions present at the termini of eukaryotic chromosomes.[4] In human cells, telomeres consist of tandem repeats of $(TTAGGG/CCCTAA)_n$ where the G-rich strand protrudes at the 3′ terminal as a single-stranded overhang of about 100−300 bases. Telomere length is reduced upon each cell replication cycle due to the end-replication effect. When the number of tandem repeats falls below a critical value, the cell stops dividing and enters a state of senescence.[5] However, the telomere 3′ overhang can serve as a substrate for the reverse transcriptase telomerase enzyme complex which maintains telomere length and plays a key role in cellular immortalization.[6] Telomerase is expressed in germ line cells and in more than 85% of cancer cells, but not at significant levels in normal somatic cells.[7] Once telomerase is inhibited or repressed, cells can divide only a limited number of times until the so-called "Hayflick" limit is reached and cells then enter a state of replicative senescence. Hence, a broad spectrum of tumor types can potentially be treated by targeting this telomere maintenance mechanism with, in principle, little cytotoxic effect on normal tissues.[8]

A well-studied approach to impair telomerase activity is to switch the G-rich human telomere overhang sequence from a linear form into a folded intramolecular G-quadruplex structure that can no longer be recognized by the RNA template of telomerase, thus preventing DNA elongation.[9] A number of G-quadruplex stabilizing molecules such as anthraquinones, porphyrins, perylenes, and acridines have been shown to inhibit telomere elongation by telomerase and several are under investigation as potential anticancer drugs.[10] In addition to the expected inhibition of telomerase, causing telomere erosion and long-term senescence, in some instances a high level of rapidly occurring senescence and apoptosis have been observed that are related to quadruplex stabilization and telomerase uncapping at the 3′ end of the telomere. These would thus substantially contribute to short-term cell death processes.[9c,d]

Anthraquinones (AQ[a]) are well-known pharmacophores with DNA-interacting properties.[11] They show preference for binding to different DNA structures depending on the positions of the appending side chains: 1,4-AQs effectively interact with duplex

* To whom correspondence should be addressed. Phone: +39 049 827 5699. Fax: +39 049 827 5366. E-mail: manlio.palumbo@unipd.it.
[†] Department of Pharmaceutical Sciences, University of Padova.
[‡] School of Biological Sciences, University of Southampton.
[§] CRUK Biomolecular Structure Group, The School of Pharmacy, University of London.

[a] Abbreviations: AA, aminoacid; AQ, anthraquinones; β-Ala, β-alanine; CHAPS, 3[(3-cholamidopropyl)dimethylammonio]-propanesulfonic acid; DIEA, diisopropylethylamine; DMEM, Dulbecco's modified Eagle medium; DMF, dimethylformamide; DMSO, dimethylsulfoxide; ED, ethylendiamine; EGTA, ethylene glycol bis(2-aminoethyl ether)-*N*,*N*,*N*′*N*′-tetraacetic acid; FAM, fluorescein; HBTU, 2-(1*H*-benzotriazole-1-yl)-1,1,3,3-tetramethyluronium hexafluoro phosphate; HTS, human telomeric sequence; Mtr, methoxytrytyl; MTT, (3-(4,5-dimethylthiazol-2-yl)-2,5-diphenyltetrazolium bromide; PCR, polymerase chain reaction; PMSF, phenylmethylsulfonyl fluoride; TBE, Tris/borate/EDTA buffer; TFA, trifluoroacetic acid; THF, tetrahydrofuran; TRAP, telomerase repeat amplification protocol; TSNT, 1-(*p*-toluenesulfonyl)-3-nitro-1,2,4-triazole.

10.1021/jm800160v CCC: $40.75
Published on Web 08/28/2008

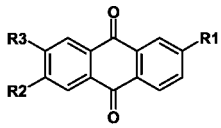

R1= - X – $(CH_2)_n$ -NH_2				
	X	**n**	**R2**	**R3**
2,6AQ-Gly	NH CO	1	R1	H
2,6AQ-βAla	NH CO	2	R1	H
2,7AQ-βAla	NH CO	2	H	R1
2,6AQ-ED	CO NH	2	R1	H
2,7AQ-ED	CO NH	2	H	R1

Figure 1. Chemical structures of the anthraquinone scaffolds used in this work. These were then conjugated to amino acids to give the final products listed in Table 1.

DNA through an intercalation process, whereas 2,6 and 2,7-AQs show a preference for triplex and quadruplex DNAs.[12] The interaction model predicts that the anthraquinone moiety should stack onto a terminal G-tetrad of a quadruplex, whereas the side chains should project into the G-quadruplex grooves.

In previous work, we introduced several amino acids at positions 1,4 of the anthracenedione system with the aim of modulating sequence selectivity in binding to quadruplex DNAs.[13] Our results showed that the presence of aminoacyl residues is responsible for sequence-selective recognition through groove interactions. Indeed, slope, charge density and pattern of potential hydrogen bonding are characteristic parameters of DNA grooves and they have been used to successfully design drugs able to recognize predefined sequences. These parameters, however, depend not only on the DNA sequence but also on the three-dimensional structure that it can form.

In the present paper, we prepared series of 2,6- and 2,7-bis-substituted anthraquinone−aminoacid conjugates as potential G-quadruplex-selective ligands (Figure 1). The amino acid residues were attached to the aromatic system through different linkers, generating a flexible connection allowing the functional groups on the side chains to properly accommodate into the grooves. We have examined the effects of changing structural parameters such as direction of the amide bond (RCONH-AQ vs RNHCO-AQ), length of the linker (one or two methylene groups between the amido-anthraquinone and the amino acid), and the nature of the conjugated amino acid in terms of hydrophobicity, charge, and steric hindrance. A total of five families of symmetrically disubstituted anthraquinone−amino acid conjugates have been synthesized and examined for G-quadruplex and duplex DNA binding by means of fluorescence melting studies and for telomerase inhibition using the TRAP assay.

Results

Chemistry. The compounds were synthesized, starting from the suitable 2,6- or 2,7-disubstituted anthracene-9,10-dione scaffold, which was connected to the desired linker and, subsequently, to the selected amino acid to ensure efficient binding to the G-quartet arrangement.[13] As a working hypothesis, we assumed that an amidic bond is the best choice to link side chains to the anthraquinone nucleus because an amide

Table 1. *Taq* Polymerase (Taq) and Telomerase (Telo) Inhibition, HTS G-Quadruplex Stabilisation (ΔT_m), and Cell Cytotoxicity (HeLa and 293T Cell Lines) Produced by the Test Anthraquinone−Aminoacyl Conjugates[e]

Scaffold	R	Taq[a] EC_{50} (μM)	Telo[a] EC_{50} (μM)	ΔT_m[b] 1 μM[d]	ΔT_m[b] 10 μM[d]	HeLa[c] IC_{50} (μM)	293T[c] IC_{50} (μM)
2,6-AQ-Gly	-H	> 40	25	0.1	3.6	76	>100
	-Phe-NH_2	> 40	> 40	0.5	0.6	n.d.	n.d.
	-Ala-NH_2	> 40	25	6.1	9.2	17	43
	-Lys-NH_2	5.0	0.8	12	>17	27	34
	-Arg-NH_2	10	0.8	9.8	22.9	89	86
	-Gly-NH_2	> 40	5	0.4	8.6	39	>100
	-Ile-NH_2	> 40	25	0.8	4.3	18	42
	-Leu-NH_2	> 40	> 40	0.7	3.8	n.d.	n.d.
	-Pro-NH_2	> 40	10	6.1	15.6	33	>100
	-Val-NH_2	> 40	> 40	0.5	6.0	n.d	n.d
2,6-AQ-βAla	-H	> 40	1.5	9.1	18.1	>100	>100
	-Phe-NH_2	> 40	> 40	0.5	4.3	n.d.	n.d.
	-Ala-NH_2	> 40	> 40	0.2	8.2	n.d.	n.d.
	-Lys-NH_2	10	0.8	6.6	17.2	100	>100
	-Arg-NH_2	10	0.8	4.8	25	100	>100
	-Ile-NH_2	> 40	> 40	0	5.7	n.d.	n.d.
	-Val-NH_2	> 40	> 40	0	6	n.d.	n.d.
2,7-AQ-βAla	-H	10	1.2	11.3	23.4	57	79
	-Phe-NH_2	> 40	> 40	0.3	7	n.d.	n.d.
	-Ala-NH_2	> 40	15	0.3	9	64	>100
	-Lys-NH_2	2.5	1.5	3	17	>100	>100
	-Arg-NH_2	4.0	4.0	0.6	13.3	n.d.	n.d.
	-Ile-NH_2	>40	>40	0.2	2.8	n.d.	n.d.
2,6-AQ-ED	-H	20	5.0	2.0	9.0	40	86
	-Phe-NH_2	> 40	> 40	0.2	1.1	n.d.	n.d.
	-Ala-NH_2	> 40	> 40	0.4	4.4	n.d.	n.d.
	-Lys-NH_2	10	0.8	7.9	15.9	100	>100
	-Arg-NH_2	10	1.5	5.2	16.4	85	>100
	-Gly-NH_2	> 40	> 40	0.3	2.9	n. d.	n. d.
	-Ile-NH_2	> 40	> 40	0.2	1.1	n. d.	n. d.
	-Leu-NH_2	> 40	> 40	0.2	1.3	n. d.	n. d.
	-Thr-NH_2	> 40	> 40	0.4	1.9	n. d.	n. d.
	-Ser-NH_2	> 40	> 40	0.3	2.5	n. d.	n. d.
2,7-AQ-ED	-H	> 40	15	3.3	12.9	100	100
	-Phe-NH_2	> 40	> 40	0.1	1.0	n.d.	n.d.
	-Ala-NH_2	> 40	> 40	0.5	3.9	n.d.	n.d.
	-Lys-NH_2	> 40	3	5.2	14.7	84	>100
	-Arg-NH_2	10	1.2	5.1	16.2	35	85
	-Gly-NH_2	> 40	> 40	0.4	3.3	n. d.	n. d.
	-Ile-NH_2	> 40	> 40	0.4	3.0	n. d.	n. d.
	-Leu-NH_2	> 40	> 40	0.3	2.7	n. d.	n. d.
	-Thr-NH_2	> 40	> 40	0.3	3.2	n. d.	n. d.
	-Ser-NH_2	> 40	> 40	0.3	2.1	n. d.	n. d.

[a] Experimental error ± 0.3 μM. [b] Experimental error ± 0.2 °C. [c] Experimental error ± 8%. [d] Drug concentration used in the melting experiments. [e] n.d., cytotoxic data referring to non-selective compounds were not determined.

Scheme 1[a]

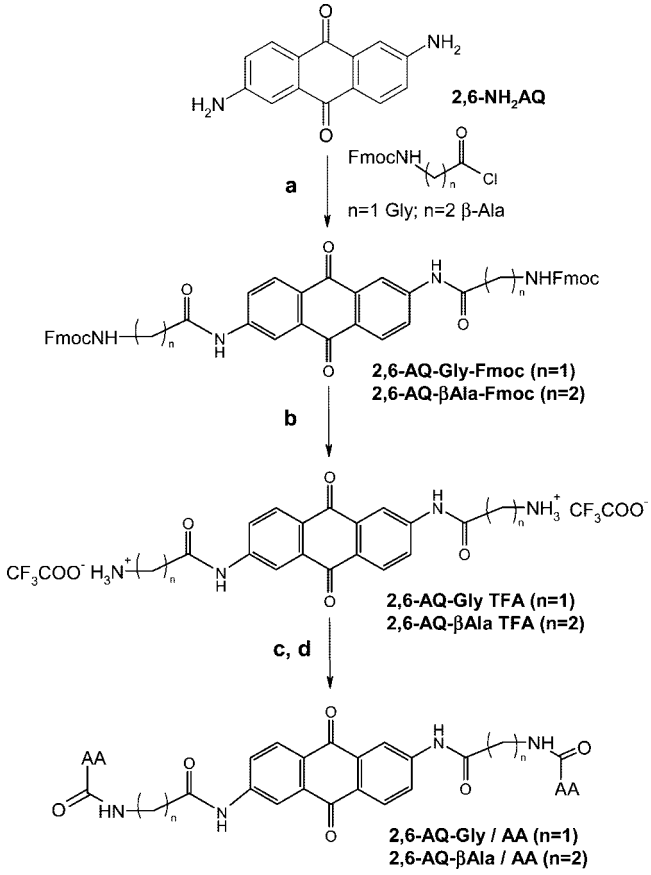

[a] Reagents and conditions. (a) Fmoc-Gly-Cl or Fmoc-βAla-Cl, THF, 7 h. (b) Piperidine, DMF, r.t. 2 h, TFA−water. (c,d) Various conditions depending on the amino acidic residue (see *Materials and Methods*). The same chemistry was used to obtain the 2,7-AQ-β Ala/AA derivatives.

would extend the planarity and aromaticity of the tricyclic system. Hence, the 2,6- and the 2,7-diaminoanthraquinone and the reciprocal 2,6- and 2,7-dicarboxyanthraquinones were obtained and used as the starting scaffolds. To obtain the desired 2,6- and the 2,7-diaminoanthraquinone derivatives, glycine or β-alanine were linked to the amino function on the anthraquinone nucleus using Fmoc protected acid chlorides. This method was preferred to the use of active esters because these amines are very poor nucleophiles. The linker was then deprotected and made to react with the free amino function of a protected amino acid. The final compounds were then obtained by deprotecting the amino functions because the presence of a protonable group is believed to be beneficial for effective interaction with the negatively charged phosphate backbone. The synthetic pathway is shown in Scheme 1.

Once prepared, the 2,6- and 2,7-dicarboxyanthraquinones were transformed into the acyl chlorides and then reacted with the amino group of 1,2-ethylenediamine protected as the Boc derivative in the presence of triethylamine. Then the Boc protection was removed using conventional methods and the resulting free amino groups were acylated with the desired amino acid protected at the amino function. In the final step, the protecting groups were removed under standard conditions. The synthesis of the derivatives of 2,6- and 2,7-dicarboxyanthraquinone is illustrated in Scheme 2.

The above approach provides simple and versatile methods to yield 2,6- and 2,7-anthraquinone derivatives (Figure 1) in which the linkers' length and nature and type of amino acid can be conveniently modulated and optimized.

Scheme 2[a]

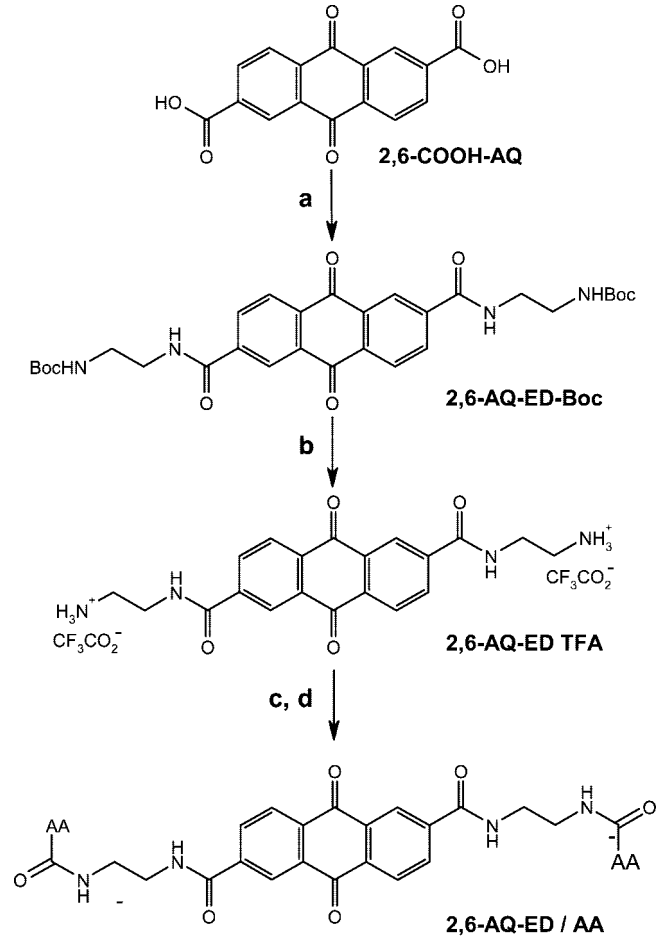

[a] Reagents and conditions. (a) $SOCl_2$, THF, reflux, 6 h, Boc-ethylenediamine, NEt_3-THF, reflux, 3 h. (b) TFA−water (90%), r.t., 1 h. (c, d) Various conditions depending on the amino acidic residue (see *Materials and Methods*). The same chemistry was used to obtain the 2,7-AQ-βAla/AA derivatives.

Fluorescence Melting Studies. Melting studies are valuable tools for assessing drug−nucleic acid interactions. In the molecular beacon approach, a fluorophore and a quencher are located along the DNA chains to produce a fluorescence change when the nucleic acid structure is altered.[14] Here, we used an oligonucleotide corresponding to four repeats of the human telomeric sequence (HTS) labeled at the 5′-end with a quencher (MethylRed) and at the 3′-end with a fluorophore (fluorescein). When the oligonucleotide folds into an intramolecular quadruplex, these groups are in close proximity and, as a consequence, the fluorescence is quenched. When DNA melts, they move further apart and a large increase in fluorescence signal occurs. This provides an excellent way of directly monitoring the thermal denaturation profile of the folded oligonucleotide. Additionally, because drug binding to a DNA structure affects its stability, hence its T_m, this approach enables rapid and effective comparison to be made of the relative G-quadruplex affinities for a range of structurally related binders.

The effects of the novel anthraquinone conjugates were systematically investigated using drug concentrations between 0.1 μM and 20 μM. Typical fluorescence melting curves for the oligonucleotide HTS in the presence of variable concentrations of poor (A) or effective ligands (B) are shown in Figure 2. All curves showed no hysteresis between the melting and annealing profiles when the rate of temperature change was 0.2 °C·min^{-1}, suggesting that the reactions are at thermodynamic

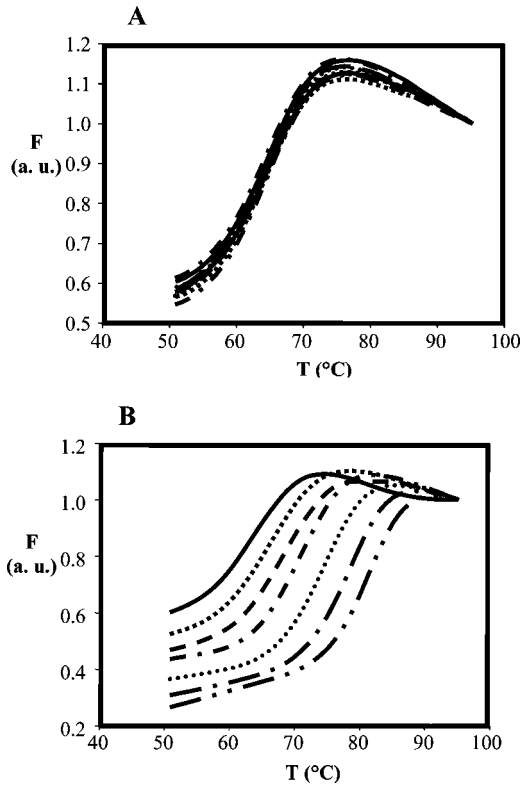

Figure 2. Fluorescence melting curves for the oligonucleotide HTS (0.25 μM) measured in the absence (solid line) or presence of increasing concentrations of 2,6-AQ-Gly-Phe (range 0.1−20 μM, (A)) and 2,6-AQ-Gly-Lys (drug concentration in an increasing order of T_m, 0.1 μM; 0.25 μM; 0.5 μM; 1.0 μM; 2.5 μM; 5.0 μM, (B)) in 50 mM potassium buffer, pH 7.4. Heating rate 0.2 °C/min.

equilibrium and that there are no kinetically controlled association or dissociation steps. There was, however, considerable hysteresis when the samples were heated at 0.1 °C•s^{-1}. The data summarized in Table 1 show that the efficiency of G-quadruplex ligand stabilization is largely affected by the nature of the aminoacyl side chains. The results obtained with the oligonucleotide HTS and the anthraquinone compounds with different linkers but without amino acids clearly showed that functionalization of the anthraquinone with β-alanine (βAla) gives the most effective spacer, followed by ethylendiamine (ED), and finally by glycine (Gly) (Figure 3). Substitution at the 2,7- position generally resulted in a slightly greater degree of G-quadruplex stabilization.

The results for the final amino acid-conjugated 2,6-AQs are given in Figure 4. Introduction of positively charged amino acids such as arginine and lysine, especially in AQ-Gly and AQ-ED scaffolds, increased the affinities of the compounds for G-quadruplexes. This is likely to be the result of enhanced electrostatic interactions between the DNA phosphate backbone and the protonated amino acid functions. On the other hand, the presence of apolar amino acids such as phenylanine, leucine, and isoleucine, reduced the ability of the βAla- and ED-anthraquinones to interact with G-quadruplexes. Indeed, among the novel conjugates, introduction of the aminoacyl residue overrides the role of the linker as the observed G-quadruplex stabilization (ΔT_m) is a function of the nature of the amino acid and is essentially constant for a given aminoacyl substituent among the different families tested here. In addition, no major differences were observed comparing 2,6 and 2,7 isomers.

Because G-quadruplex binding preference over the canonical B DNA structure represents further useful information to define

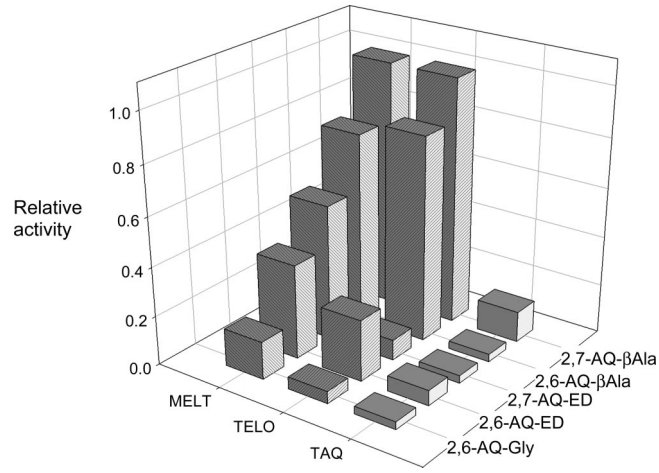

Figure 3. *TAQ* polymerase inhibition (TAQ), telomerase inhibition (TELO), and G-quadruplex stabilization (MELT) induced by the anthraquinone scaffolds used in this work. Data were normalized with reference to 2,7-AQ-βAla. G-quadruplex stabilization refers to oligonucleotide HTS in 50 mM potassium buffer, pH 7.4, 10 μM ligand.

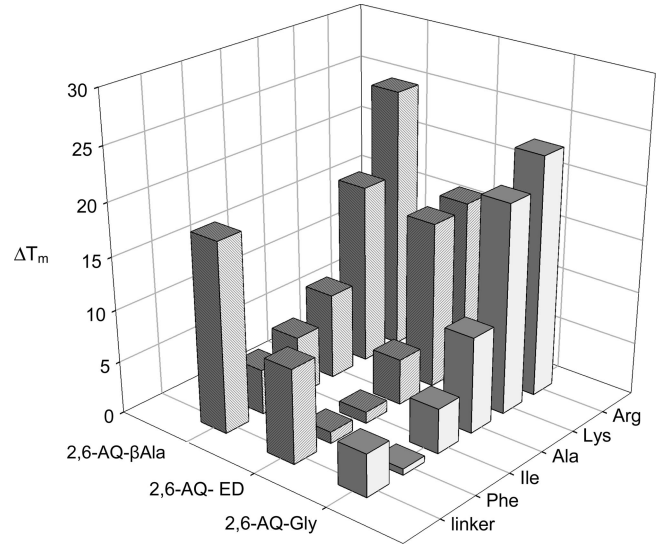

Figure 4. Stabilization (ΔT_m) induced by the test anthraquinones (final concentration: 10 μM) on the G-quadruplex structure formed by the oligonucleotide HTS in 50 mM potassium buffer, pH 7.4.

the potential of these new compounds as effective drugs, we also examined the interference of peptidyl anthraquinones with the melting of a double-stranded sequence. Although we observed a general shift of the duplex melting toward higher temperatures, the effects are in all cases much less significant than those reported for G-quadruplex stabilization. Hence, the test compounds show a clear-cut preference for the telomeric G-quadruplex arrangement.

Telomerase Inhibition. All aminoacyl−anthraquinones were evaluated for their ability to inhibit human telomerase in a modified cell-free telomerase repeat amplification protocol (TRAP) test.[15] As a first step, all new conjugates were tested at concentrations ranging from 20 nM to 40 μM for their ability to inhibit *Taq* polymerase because a PCR DNA amplification step is used in the TRAP assay and drug interference at this level can lead to false positive results. Thus, TRAP assays were performed at concentrations lower than those inhibiting *Taq* polymerase. Typical results on the inhibition of the two enzymes are reported in Figure 5 and the IC_{50} values are given in Table 1.

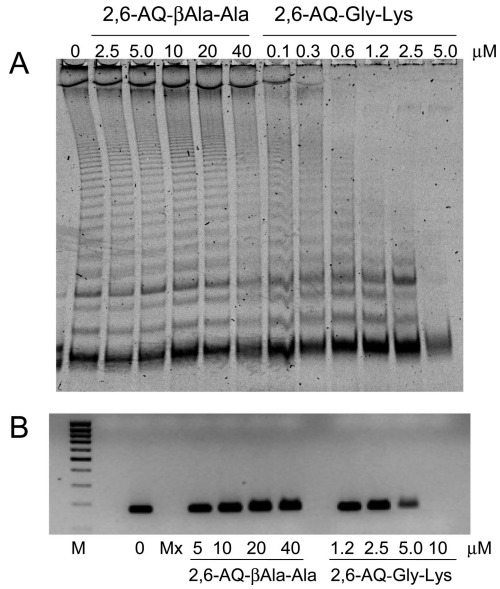

Figure 5. Representative experiments for the determination of Telomerase and *Taq* polymerase inhibitory properties by the peptidyl anthraquinone derivatives. (A) TRAP assay performed with increasing concentrations of 2,6-AQ-βAla-Ala and 2,6-AQ-βAla-Lys as indicated. (B) Inhibition of *Taq* polymerase DNA amplification reaction in the presence of increasing concentration of the above anthraquinones as indicated. M refers to molecular weight markers, 0 and MX to the amplification reaction performed in the absence of drug and in the presence of 10 mM Mitoxantrone respectively.

Considering the AQ scaffolds, the most active derivatives are the 2,6- and 2,7-AQ-βAla compounds (EC_{50} of 1.25 μM) followed by 2,6- and 2,7-AQ-ED (EC_{50} of 5 and 15 μM, respectively). 2,6-AQ-Gly inhibits telomerase with an EC_{50} > 25 μM.

For the βAla derivatives, although they have the same potency against telomerase, they have distinct *Taq* polymerase inhibition abilities, 2,7-AQ βAla being more efficient. As a result, the concentration window for selective telomerase inhibition is substantially reduced for the 2,7-disubstituted analogue in comparison with its 2,6- isomer (Figure 4).

For amino acid-conjugated compounds, the *Taq* polymerase inhibition assay revealed that only derivatives with arginine and lysine interfere with enzyme activity (at 5−10 μM). The other compounds do not inhibit *Taq* polymerase at the tested concentrations. As far as telomerase inhibition, most of the derivatives bearing apolar residues (Val, Leu, Ile, Phe) are inactive up to 40 μM, independent of the linker structure. In a few instances, introduction of apolar amino acids retains activity, although to an extent comparable to or lower than the corresponding scaffolds (2,6-AQ-Gly-Ala, 2,6-AQ-Gly-Ile, 2,6-AQ-Gly-Val). Notably, 2,6-AQ-Gly-Gly (EC_{50} of 5 μM) and 2,6-AQ-Gly-Pro (EC_{50} of 10 μM) showed lower EC_{50} values than the corresponding 2,6-AQ-Gly derivative (EC_{50} of 25 μM).

For all families of derivatives, introduction of Lys or Arg residues in the side chains results in optimal telomerase inhibition with EC_{50} values in the low μM range (0.8−3 μM). Again, the nature of the linker is less important when amino acids are coupled. Indeed, for conjugates with a given amino acid, comparable telomerase inhibition was observed irrespectively of the nature of the linker or of the position (2,6- vs 2,7-) of the side chains.

All examined compounds were able to inhibit telomerase at concentrations about 10-fold lower than those required for *Taq* polymerase inhibition.

We should add that the telomerase inhibitory values reported here should be taken to be relative values and do not take account of possible effects involving ligand interfering with the PCR step in the TRAP assay, as has been recently demonstrated.[16] This would lead to overestimating the telomerase inhibitory potency of the test drugs. However, considering that the temperature at which elongation is carried out is well above the T_m of the HTS G-quadruplex and the primers used are not able to fold into G-quadruplexes, we suggest that the possibility of the above effects occurring is minimized. This is supported by experiments in which the anthraquinone conjugates added just prior to the PCR amplification step showed at least a 4-fold increase in the apparent EC_{50} for telomerase inhibition.

Cell Cytotoxicity. The results relative to cell cytotoxicity on the human cancer cell lines HeLa and 293T are reported in Table 1. Both cell lines constitutively express telomerase,[17] hence they are useful to determine any inhibitory effect caused by the test peptidyl−anthraquinones. The evaluation was performed only for those compounds exhibiting preferential telomerase vs *Taq* polymerase inhibition, hence promising in terms of selectivity for the target enzyme.

Indeed, the new compounds are poorly cytotoxic in the short term experiments, which is consistent with the expectation of delayed cytotoxicity due to slow telomere erosion brought about by effective telomerase inhibitors. In general, HeLa cells appear to be more sensitive than 293T cells to the test anthraquinones. It is worth recalling that Mitoxantrone, used as a reference drug in our tests, was substantially more cytotoxic, as it exhibited IC_{50} values below 0.1 μM against both above cell lines. When comparing the cytotoxicity data, it is immediately evident that they do not correlate either with telomerase inhibition or with G-quadruplex stabilization. Overall, among efficient G-quadruplex ligands, the more hydrophilic Lys- and Arg-containing conjugates seem to be less cytotoxic. Low short-term cytotoxicity can be reasonably expected for derivatives acting on telomerase-related targets as telomere erosion requires a number of cell cycles to produce cell death. In addition to the proposed mechanism of action, poor cell killing ability might be due to less effectual cell uptake of the most highly charged compounds.

Senescence Induction in HeLa Cells. To assess delayed toxicity, we performed cell senescence determinations using histochemical staining of β-galactosidase activity at pH 6.0. Representative results are shown in Figure 6. Interestingly, HeLa cells treated for 144 h with the most effective G-quadruplex stabilizers showed intense staining using drug concentrations at which telomerase was inhibited. This represents a clear evidence of the onset of a senescence phenotype in an otherwise immortal cell line. To confirm a differential effect due to drug treatment, poor G-quadruplex binders caused remarkably reduced staining, whereas untreated controls did not exhibit appreciable staining, which proves that the immortal phenotype is preserved in the absence of drugs (Figure 6). The observed response indirectly indicates that the charged compounds can be adequately internalized into HeLa cells.

Discussion

Anthraquinones (AQ) with side chains at the 2,6- and 2,7-positions have been previously found to bind preferentially to G-quadruplex structures.[12d] The present study extends these observation to a small library of anthraquinone-amino acid conjugates symmetrically disubstituted at positions 2,6 or 2,7. To clarify the structural requirements to optimize interactions with the human telomeric G-quadruplex, we took into account:

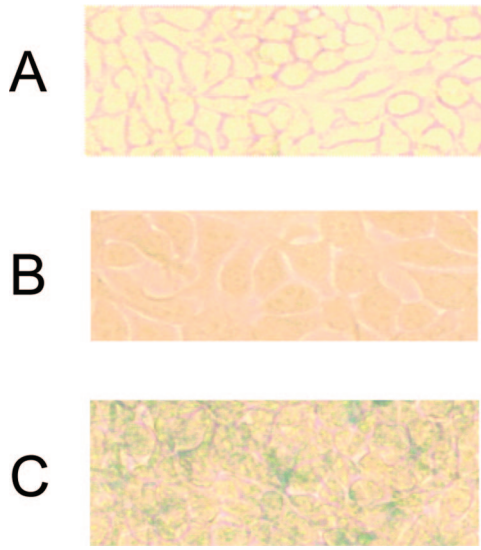

Figure 6. β-Galactosidase staining at pH 6 following 144 h treatment of HeLa cells with no added drug (A), with 2.5 μM 2,6-AQ-Gly-Phe (B), and with 2.5 μM 2,6-AQ-Gly-Lys (C).

- Relative positions of the side chains (2,6-AQs vs 2,7-AQs).
- Direction of the amide linkage between the linker and the anthraquinone (amide or "reversed" amide).
- Length of the linker.
- Charge, lipophilicity and bulkiness of the amino acid in the side chains.

This allowed us to optimize the nature of the linker and the nature and location of the side chains for telomeric G-quadruplex recognition and telomerase inhibition. Several of the novel compounds effectively stabilize the G-quadruplex folding of the human telomeric sequence, although to remarkably different extents. Notably, they bind to duplex DNA with substantially lower affinity, hence confirming their preference for the G-quadruplex arrangement, which is a basic requirement to develop telomere-directed new drugs.

The following equation can be made to relate $\Delta T_m/T_m$ to the stability constant K of drug−nucleic acid (G-quadruplex) interaction:

$$\Delta T_m/T_m = T^0(R/n\Delta H_{wc}) \ln(1 + K\alpha) \quad (1)$$

where T^0 is the melting temperature of DNA alone, T_m is the melting temperature in the presence of saturating amounts of the drug, ΔH_{wc} is the enthalpy of DNA melting, R is the gas constant, K is the drug binding constant at the T_m value, and α is the free drug activity.[18]

If drug potency against telomerase ($1/EC_{50}$) is directly related to the amount of G-quadruplex complex formed, which, in turn, is proportional to K in the presence of excess drug, then, in the reasonable hypothesis that $K\alpha \gg 1$, we should find a linear relationship between $\Delta T_m/T_m$ and $\ln EC_{50}$. Indeed, a satisfactory correlation between these two parameters is found for all compounds examined in this work as shown in Figure 7 using the data presented in Table 1. This finding supports telomerase inhibition as being directly related to ligand affinity for G-quadruplex structure for the aminoacyl anthraquinone family. As a consequence, structure−activity relationships based on enzymatic activity parallel those obtained using the G-quadruplex stabilization. Our data indicate that:

- The shift of the side chains from position 2,6 to 2,7 does not alter significantly the G-quadruplex stabilization properties nor does it appreciably affect the enzyme inhibition activity.

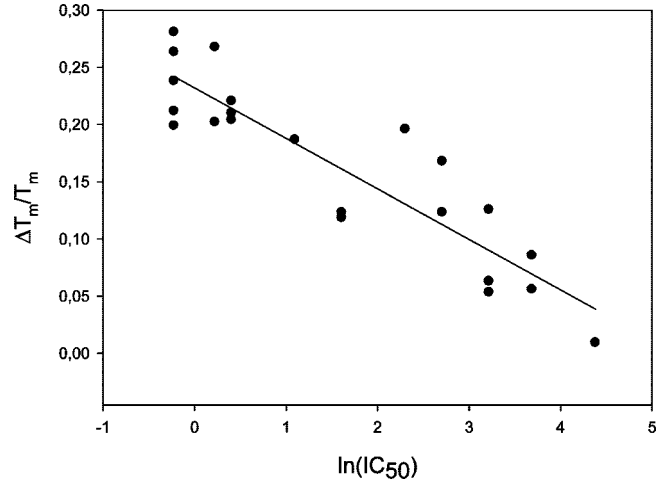

Figure 7. Correlation between the thermal stabilization ($\Delta T_m/T_m$) of HTS G-quadruplex by test derivatives and their EC_{50} values for telomerase inhibition.

This suggests that there is a degree of flexibility in the geometry of the drug−DNA complex.

- Derivatives having the NH group of the amide linker bound to the AQ ring are superior G-quadruplex binders/telomerase inhibitors compared to those with the C═O group facing the aromatic system. This fact could be explained by changes in the coplanarity of the amide bond with the aromatic system in the two derivatives, βAla-AQ being more planar than ED-AQ. As anthraquinone binding to G-quadruplexes occurs through stacking interactions with the G-tetrads, the more extended planar system present in βAla enables more favorable interactions to take place.
- AQs functionalized with glycine apparently are even less efficient than βAla and ED derivatives. This can be linked to the reduced distance between the positively charged amino terminal group and the aromatic core. Indeed, elongation of the chain of the 2,6-AQ-Gly derivative with a further Gly residue produces a remarkable increase in complex stability and in biochemical activity.
- The importance of the ionic interactions in the recognition process has been demonstrated. The presence of uncharged groups in the amino acid side chains reduces the recognition of folded structures and decreases activity against telomerase. This effect is evident in the presence of amino acid substituents characterized by steric hindrance such as phenylalanine. On the other hand, compounds containing Lys and Arg residues in the side chains, capable of forming efficient ionic interactions with the phosphate backbone, are the most effective derivatives. Thus, the presence of more than two protonated functions per molecule at physiological conditions appears to represent an important determinant of G-quadruplex activity.

Additionally, conjugation of the amino acid to the basic scaffold induces a leveling off of the differences among the three linkers used in this work. In particular, the better performances due to the introduction of basic amino acids are recorded in the presence of Gly or ED linker but not in the case of β-Ala, which is remarkably effective per se. If we take into account the concentration window between *TAQ* polymerase and telomerase inhibition, the 2,6-AQ-βAla isomer appears to be the best scaffold to work with. As a future development, further elongation of the side chains with more complex peptide sequences is in progress.

It is encouraging to observe the relative lack of short-term cytotoxicity exhibited by the most promising derivatives, which correlates well with a slow induction of senescence

by telomerase inhibitors. Moreover, anthraquinone conjugates similar to those presented here, but characterized by 1,4 disubstitution, proved to be much more cytotoxic, exhibiting IC_{50} values in the low micromolar range and comparable to Mitoxantrone in the HeLa cell line.[19] This shows that it is not simply the chemical constitution of the side chains that renders them nontoxic on short term but especially their location on the anthraquinone scaffold, which modulates the recognition of DNA and DNA-processing enzymes.

Cell senescence determinations confirm delayed toxicity induced by the Lys- and Arg-containing AQ derivatives, a behavior expected for efficient G-quadruplex binders and telomerase inhibitors. Although measurements on telomere shortening and uncapping are required before drawing final conclusions, our results are clearly suggestive of a telomerase-mediated mechanism of toxicity.[20,21] However, because our effective compounds exhibit affinity for G-quadruplex arrangements other possible telomere-independent genomic targets can be involved in drug action. In fact, a large number of putative G-quadruplex forming sequences have been identified in the human chromosome, some of which could efficiently interact with peptidyl anthraquinones.[22]

In conclusion, our results suggest that the novel anthracenedione conjugates presented in this work can be considered as useful leads in view of a selective antiproliferative pharmacological approach.

Materials and Methods

Anthraquinones. Chemicals, reagents and solvents, were purchased from Aldrich or Fluka and used without further purification. Amino acids were from Novabiochem. ^{1}H and ^{13}C NMR spectra were recorded on a Bruker AMX300 spectrometer in deuterated methyl sulfoxide (DMSO-d_6) from Cambridge Laboratory, and chemical shifts are in ppm. Chromatography and flash chromatography were performed using silica gel Merck 60 (70−230 mesh) and Merck 60 (40−63 μm) respectively. TLC plates were also from Merck: Merck 60 F-254, 0.25 mm precoated plates. Melting points were determined using a Gallenkamp apparatus in capillary tubes and are uncorrected. Elemental analysis (C, H, N) was performed by the Microanalytical Laboratory of the Department of Pharmaceutical Sciences of the University of Padova on a Carlo Erba 1016 elemental analyzer, and the observed values are within 0.40% of the calculated values. Exact masses (HRMS) were obtained using a Mariner API-TOF (Perseptive Biosystems Inc., Framingham MA 01701), and found and calculated *m/z* values are given. The starting anthraquinones were obtained as described previously.[13]

Within the experimental part AQ stands for anthraquinone, Gly for glycine, β-Ala for β-alanine, and ED for 1,2-ethylenediamine and, in the general procedures, glycine, β-alanine, and ED are collectively called "linker."

General Procedure for the Preparation of 2,6-Bis-[*N*-(2-Fmoc-amino)-acetamide]anthracene-9,10-dione, Scheme 1 (2,6-AQ-Gly-Fmoc). Commercial 2,6-diamino-anthraquinone (0.793 g, 3.33 mmol) was suspended in dry THF (120 mL) and Fmoc-Gly-Cl (3.15 g, 10 mmol) was added. The mixture was heated to reflux for 7 h, and a color change was observed from dark red to orange. The product was collected as precipitate by centrifugation from the cooled solution, washed with HCl 1 M and Et_2O, and dried. 2,6-AQ-Gly-Fmoc was obtained as a red-orange powder (2.53 g, 94%). ^{1}H NMR (DMSO-d_6): δ 10.65 (s, 2H), 8.44 (s, 2H), 8.17 (d, J = 8.3 Hz, 2H), 8.06 (d, J = 8.3 Hz, 2H), 7.89 (d, J = 7.9 Hz, 4H), 7.75−7.67 (m, 6H), 7.11−7.46 (m, 8H), 4.31 (d, J = 7.4 Hz, 4H), 4.25 (t, J = 7.4 Hz, 2H), 3.38 (d J = 5.6 Hz, 4H). HRMS $C_{48}H_{36}N_4O_8$: 797.8433, M + H requires 797.8431.

General Procedure for the Preparation of 2,6-Bis-(2-amino-acetamide)-anthracene-9,10-dione ditrifluoroacetate, Scheme 1 (2,6-AQ-Gly TFA). 2,6-AQ-Gly-Fmoc (2.67 g, 7.84 mmol) was dissolved in DMF (76 mL) and piperidine (4 mL). The solution was stirred at r.t. for 2 h and then poured in Et_2O. The free base was collected by centrifugation of the suspension, washed with Et_2O and water, and dried. The free base was dissolved in TFA/water 9/1 (20 mL), stirred at r.t. for 2 h, and then poured in Et_2O. The product was collected by centrifugation, washed with Et_2O and water, and dried. 2,6-AQ-Gly TFA was obtained as red-orange solid (2.67 g, 90%). ^{1}H NMR (DMSO-d_6): δ 11.14 (bs, 2H), 8.72 (d, J = 1.9 Hz, 2H), 8.25−8.21 (m, 8H), 8.04 (dd, J = 8.7 and 1.9 Hz, 2H), 3.90 (s, 4H). ^{13}C NMR (DMSO-d_6): δ 181.1, 165.8, 143.6, 134.3, 128.6, 128.4, 123.6, 115.8, 41.2. HRMS $C_{18}H_{16}N_4O_4$: 353.129, M + H requires 353.124.

General Procedure for the Preparation of 2,6- or 2,7-Bis-[*N*-(3-Fmoc-amino)-propionamide]anthracene-9,10-dione, Scheme 1 (2,6-AQ-βAla-Fmoc or 2,7-AQ-βAla-Fmoc). Commercial 2,6-diamino-anthraquinone (0.40 g, 1.7 mmol) was suspended in dry THF (60 mL) and Fmoc-βAla-Cl (1.36 g, 4.1 mmol) was added. The mixture was heated to reflux for 7 h and a color change from dark red to orange was observed. The product was collected by centrifugation from the cooled solution and washed with 1 M HCl and acetone. 2,6-AQ-βAla-Fmoc was obtained as a red-orange powder (1.32 g, 95%). ^{1}H NMR (DMSO-d_6): δ 10.59 (s, 2H), 8.50 (d, J = 1.8 Hz, 2H), 8.15 (d, J = 8.3 Hz, 2H), 8.06 (dd, J = 8.3 and 1.8 Hz, 2H), 7.86 (dd, J = 7.4 and 0.9 Hz, 4H), 7.68 (dd, J = 7.4 and 0.9 Hz, 4H), 7.46 (t, J = 5.4 Hz, 2H), 7.38 (dt, J = 7.4 and 0.9 Hz, 4H), 7.29 (dt, J = 7.4 and 0.9 Hz, 4H), 4.27 (d, J = 6.4 Hz, 4H), 4.21 (t, J = 6.5 Hz, 2H), 3.33 (t, J = 6.3 Hz, 4H), 2.59 (t, J = 6.2 Hz, 4H). ^{13}C NMR (DMSO-d_6): δ **2,6-isomer** 181.4, 144.1, 134.6, 128.8, 128.2, 123.2, 117.9; **2,7-isomer** 184.9, 180.9, 144.7, 134.8, 131.2, 128.3, 123.1, 120.3; **2,6- and 2,7- side chains** 169.1, 155.9, 142.5, 140.9, 127.8, 127.3, 125.4, 76.1, 46.9, 36.9, 35.7.

General Procedure for the Preparation of 2,6- or 2,7-Bis-(3-amino-propionamide)-anthracene-9,10-dione ditrifluoroacetate, Scheme 1 (2,6-AQ-βAla TFA or 2,7-AQ-βAla TFA). 2,6-AQ-βAla-Fmoc (0.84 g, 1.0 mmol) was dissolved in DMF (54 mL) and piperidine (6 mL). The solution was stirred 2 h at r.t. and then poured in Et_2O. The free base was collected by centrifugation of the resulting suspension, washed with Et_2O and water, and dried. The free base was dissolved in TFA−water 9/1 (20 mL), stirred 2 h at r.t. and then poured in Et_2O. The product was collected by centrifugation, washed with Et_2O and water, and dried. 2,6-AQ-βAla TFA was obtained as red-orange solid (0.56 g, 92%). ^{1}H NMR (DMSO-d_6): δ 10.76 (s, 2H), 8.53 (d, J = 1.8 Hz, 2H), 8.18 (d, J = 8.3 Hz, 2H), 8.01 (dd, J = 8.3 and 1.8 Hz, 2H), 7.75 (bs, 6H), 3.12 (m, 4H), 2.77 (t, J = 6.5 Hz, 4H). ^{13}C NMR (DMSO-d_6): δ **2,6-isomer** 181.6, 169.7, 144.6, 134.6, 128.8, 128.4, 123.8, 116.2, 34.9, 33.7; **2,7-isomer** 184.9, 180.9, 144.7, 134.8, 128.8, 128.4, 123.8, 116.2; **2,6- and 2,7- side chains** 169.7, 34.9, 33.7. HRMS $C_{20}H_{20}N_4O_4$: 191.08, M + 2H requires 191.08.

General Procedure for the Preparation of 2,6- or 2,7-Dicarboxyanthraquinone Chloride. 2,6- (or 2,7-) Dicarboxyanthraquinone (0.70 g, 2.4 mmol) was suspended in dry THF (150 mL). To the suspension was added freshly distilled thyonyl chloride (1.73 mL, 23.8 mmol) and the reaction mixture refluxed 7 h, by which time a clear solution was observed. The excess solvents were removed in vacuo and the residue was washed with chloroform. The 2,6- (or 2,7-) dicarboxyanthraquinone chloride was used without any further purification or characterization directly in the next reaction (assuming a quantitative yield).

General Procedure for the Preparation of 2,6- or 2,7-Bis-(Boc-amino-ethyl-carbamoyl)-anthracene-9,10-dione (2,6- or 2,7-AQ-ED TFA). 2,6- (or 2,7-) Dicarboxyanthraquinone chloride (0.48 g, 1.5 mmol) was suspended in dry THF (35 mL) and triethylamine was added (0.42 mL, 3 mmol). Then a solution of mono-*N*-(*tert*-butoxycarbonyl)ethylenediamine (0.48 g, 3 mmol) in dry THF (5 mL) was added. The mixture was refluxed for 3 h and then cooled to 0 °C. 2,6- (or 2,7-) AQ-ED-Boc was collected by centrifugation and washed with water and dried in vacuo to give the 2,6-AQ-ED-Boc (0.64 g, yield 73%) or 2,7-AQ-ED-Boc (0.68 g, yield 78%). No further purification of the products was required. ^{1}H NMR (DMSO-d_6): δ 8.95 (bs,2H), 8.66 (s, 2H), 8.32 (d, J = 7.7 Hz,

2H), 8.29 (d, $J = 7.7$ Hz, 2H), 6.95 (bs, 2H), 3.33 (m, 4H), 3.16 (m, 4H), 1.37 (s, 18H). ^{3}C NMR (DMSO-d_6): δ **2,6-isomer** 182.5, 166.5, 139.4, 137.0, 136.5, 135.4, 134.1, 128.3; **2,7-isomer** 182.5, 182.2, 166.7, 136.6, 136.4, 135.4, 134.0, 128.3 28.6; **2,6- and 2,7-side chains** 156.6, 77.2, 43.7, 42.1.

General Procedure for the Preparation of 2,6- or 2,7-Bis-(2-ammonium-ethyl-carbamoyl)-anthracene-9,10-dione Bis-trifluroacetate (2,6-AQ-ED TFA or 2,7-AQ-ED TFA). 2,6- (or 2,7-) AQ-ED-Boc (500 mg, 0.86 mmol) was dissolved in trifluoroacetic acid−water 9/1 (50 mL). The solution was stirred at r.t. for 1 h and then poured in water. The resulting solid was collected by filtration and washed with water, dried in vacuo, and washed with Et_2O. The solid product was dried in vacuo for 1 h to give 2,6- (or 2,7-) AQ-ED TFA salt as a pale-yellow solid (quantitative yield). ^{1}H NMR (DMSO-d_6): δ 9.13 (t, $J = 5.3$ Hz, 2H), 8.69 (d, $J = 1.3$ Hz, 2H), 8.38 (dd, $J = 8.2$ and 1.5 Hz, 2H), 8.33 (d, $J = 8.2$ Hz, 2H), 8.02 (bs, 6H), 3.62−3.55 (m, 4H), 3.13−3.01 (m, 4H). ^{13}C NMR (DMSO-d_6): δ **2,6-isomer** 181.8, 165.3, 139.0, 134.7, 133.1, 133.0, 127.1 125.7, 38.4, 37.3; **2,7-isomer** 183.4, 166.9, 140.6, 136.4, 134.7, 128.7, 127.3, 40.0, 38.9. HRMS $C_{20}H_{20}N_4O_4$: 191.085, M + 2H requires 191.081.

General Procedure for the Coupling between 2,6- (or 2,7-) AQ-linker TFA and Boc protected, OSu Activated Amino Acids (Boc-AA-OSu) Followed by Boc Removal. Method A. 2,6- (or 2,7-) AQ-linker TFA (0.10 mmol) was dissolved in dry DMF (2 mL), followed by DIEA (0.1 mL, 0.57 mmol) and Boc-AA-OSu (0.60 mmol). The solution was stirred at r.t. under N_2 for 10 h and then poured in Et_2O and centrifuged. The solid obtained was washed with Et_2O and then water and dried in vacuo. The raw product 2,6- (or 2,7-) AQ-linker-AA-Boc) was used in the next step without any further purification.

To remove the Boc-protecting group, the 2,6- (or 2,7-) AQ-linker-AA-Boc was dissolved in TFA−water 9/1 (3 mL), stirred at r.t. for 4 h, and then poured in Et_2O, and the resulting suspension was centrifuged. The solid obtained was washed with Et_2O and then dried in vacuo.

General Procedure for the Coupling between 2,6- (or 2,7-) AQ-linker TFA and Boc-Protected Amino Acids (Boc-AA-OH), Followed by Boc Removal. Method B. 2,6- or (2,7-) AQ-linker TFA (0.10 mmol) was dissolved in dry DMF (2 mL), followed by DIEA (0.1 mL, 0.57 mmol), Boc-AA-OH (0.25 mmol), and HBTU (95 mg, 0.25 mmol). The solution was stirred at r.t. under N_2 for 10 h and then poured in Et_2O and centrifuged. The solid obtained was washed with Et_2O and water, dried in vacuo, and used in the next step without any further purification.

To remove the Boc-protecting group, the 2,6- (or 2,7) AQ-linker-AA-Boc from the first step was dissolved in TFA−water 9/1 (3 mL) and stirred at r.t. for 4 h and then poured in Et_2O, and the resulting suspension was centrifuged. The solid obtained was washed with Et_2O and then dried in vacuo.

General Procedure for the Coupling between 2,6- (or 2,7-) AQ-linker TFA and Arginine, Followed by Deprotection and Formation of TFA Salt. Method C. 2,6- (or 2,7-) AQ-linker TFA (0,10 mmol) was dissolved in dry DMF (2 mL), and DIEA (0.1 mL, 0.57 mmol), Fmoc-Arg(Mtr)-OH (152 mg, 0.25 mmol), and HBTU (95 mg, 0.25 mmol) were added. The resulting solution was stirred at r.t. under N_2 for 10 h, then poured in Et_2O and centrifuged. The solid obtained was washed with Et_2O and the product 2,6- (or 2,7-) AQ-linker-Arg(Mtr)-Fmoc was dried in vacuo and used in the next step without any further purification.

To remove the Fmoc- protecting group, the 2,6- (or 2,7-) AQ-linker-Arg(Mtr)-Fmoc was dissolved in DMF−piperidine 9/1 (4 mL) and stirred at r.t. for 6 h and then poured in Et_2O and centrifuged. The solid obtained was washed with Et_2O and water and then dried in vacuo. Subsequently, to remove the Boc-protecting group, the 2,6- (or 2,7-) AQ-linker-Arg(Mtr) was dissolved in TFA−thioanisole 19/1 (3 mL) and stirred at r.t. for 8 h and then poured in Et_2O, and the resulting suspension was centrifuged. The solid obtained was washed with Et_2O and dried in vacuo.

Synthetic Oligonucleotides. The human telomeric sequence tetramer HTS (5′MeRed-AGGGTTAGGGTTAGGGTT AGGGT-FAM 3′) and the sequence used for duplex studies (5′ FAM-AGACATAAGAGCATGAGAA 3′/5′ TCTCATGCTCTTATGTCT-MeRed 3′) were synthesized and HPLC purified by Oswel Research Products Ltd. (Southampton, UK) and contain, where indicated, fluorescein (FAM) at the 5′-end of the oligonucleotide and methyl red (MeRed) at 3′-end.

The DNA oligonucleotides used for *Taq* polymerase inhibition assay and TRAP assay were synthesized by Eurogentec (Belgium) and used with no further purification (TS:5′-AATCCGTCGAG-CAGAGTT-3′;ACX: 5′-GTGCCCTTACCCTTACCCTTACCCTAA-3′; TSNT:5′ AATCCGTCGAGCAGAGTTAAAAGGCCGAGA-AGCGAT-3′;NT:5′-ATCGCTTCTCGGCCTTTT-3′;Tup:5′-TGAGGATC-CGCCTGGACAGCATGG-3′;Tdown: 5′-GTCGAATTCTCGGCGA-GAAGCAGG-3′).

Taq Polymerase Assay. To meet proper working conditions, compounds were assayed against *Taq* polymerase reaction by using pBR322 (2.5 ng) as a DNA template and appropriate primer sequences Tup and Tdown (0.5 μM) to amplify the 906−1064 sequence of plasmid by PCR. The reaction was carried out in a Perkin-Elmer thermocycler performing 25 cycles of: 30 s at 94 °C, 30 s at 65 °C, and 30 s at 72 °C. The reaction products were resolved on a 2% agarose gel in TBE (89 mM Tris base, 89 mM boric acid, 2 mM Na_2EDTA) and stained by ethidium bromide.

Telomerase Activity Assay (TRAP assay). An aliquot of 5×10^6 JR8 cells in exponential phase of growth was pelleted and lysed for 30 min on ice using 100 μL of 0.5% CHAPS, 1 mM EGTA, 25% 2-mercaptoethanol, 1.74% PMSF, and 10% w/v glycerol. The lysate was centrifuged at 13000 rpm for 30 min at 4 °C and the supernatant collected, stored at −80 °C, and used as the telomerase source.

Telomerase activity was assayed using a modified telomere repeat amplification protocol (TRAP) assay. Briefly, an appropriate primer TS (5′-AATCCGTCGAGCAGAGTT-3′; Biosense) have been 5′-labeled with [γ-^{32}P]ATP and T4 polynucleotide kinase. After enzyme inactivation (85 °C for 5 min), a 50 μL TRAP reaction mix (50 μM of dNTPs, 0.2 μg of labeled TS, 0.1 μg of return primer ACX, 500 ng of protein extract, 2 U *Taq* polymerase) was prepared in the presence/absence of increasing drug concentration in 20 mM Tris-HCl pH 8.3, 68 mM KCl, 1.5 mM $MgCl_2$, 1 mM EGTA, 0.05% v/v Tween- 20. According to (41), an internal control template (0.01 mmol TSNT) with its return primer (1 ng NT) were added to the reaction mixture. Then, telomerase elongation step has been performed (30 min at 30 °C), followed by a PCR amplification step (30 cycles of: 30 s at 37 °C and 30 s at 58 °C). The reaction products were loaded onto a 10% polyacrylamide gel (19:1) in TBE 0.5X. Gels were transferred to Whatman 3MM paper, dried under vacuum at 80 °C, and read using a phosphorimager 840 (Amersham). Measurements were made in triplicate with respect to a negative control run using the equivalent TRAP-PCR conditions but omitting the protein extract, thus ensuring that the ladders observed were not due to artifacts of the PCR reaction.

Fluorescence Melting Studies. The melting temperature of the quadruplex formed by the telomere-based sequence HTS in the presence/absence of ligands, was determined by fluorescence melting experiments performed in a Roche LightCycler, using an excitation source at 488 nm. The changes in fluorescence emission were recorded at 520 nm.

Melting experiments were performed in a total volume of 20 μL containing 0.25 μM quadruplex forming oligonucleotide HTS and variable concentrations of tested derivatives in LiP buffer (10 mM LiOH; 50 mM KCl pH 7.4 with H_3PO_4). Mixtures were first denatured by heating to 95 °C at a rate of 0.5 °C·min^{-1} and keeping this temperature for 5 min. They were then cooled to 30 °C at a rate of 0.5 °C·min^{-1}. Recordings were taken during both the melting and annealing reactions to check for hysteresis. These slow rates of heating and cooling were achieved by changing the temperature in 1 °C steps, leaving the samples to equilibrate for 2 min before each fluorescence reading. Considerable hysteresis was observed with faster rates of heating and cooling (0.1 °C·min^{-1}) for the quadruplex (but not duplex) melting curves.

T_m values were determined from the first derivatives of the melting profiles using the Roche LightCycler software.

Cell Cultures and Toxicity Assays. HeLa (human hepitelial) and 293T (human renal epithelial) cell lines were maintained in DMEM medium supplemented with 10% heat-inactivated fetal calf serum, 50 U/mL of penicillin G, and 50 μg/mL of streptomycin at 37 °C in humidified atmosphere and 5% of CO_2.

To evaluate toxic profiles of the potential antitelomerasic compounds, MTT assays were performed as described: cells were plated in 96 well plates at 10000 cells/well and cultured overnight. Afterward, compounds were added in triplicate, and plates were incubated in presence of the drug for 96 h. At the end of this period, MTT was added to a final concentration of 0.8 mg/mL, and two additional hours of incubation were performed. After that, medium was aspirated carefully and 150 μL of DMSO were added per well. Soluble formazan salts were homogenated by manual pipetting and absorbance at 540 nm was read. Curves consisted in eight serial dilutions in triplicate in each case, and results were analyzed as sigmoidal dose−response curves.

Cell Senescence Assay. HeLa cells were plated in 6-well plates at 10000 cells/well and cultured overnight. Afterward, compounds were added in triplicate (2.5 μM) and plates were incubated in presence of the drug for 144 h. Every 72 h, the medium was changed and new drug was added. At the end of the treatment, medium was removed and cells were washed once with 1 mL of PBS and fixed with 1 mL of 2% formaldehyde, 0.2% glutaraldehyde in PBS for 15 min at room temperature. After another washing step with PBS, cells were stained with 1 mL of 37.2 mM citric acid/sodium phosphate (pH 6.0), 140 mM NaCl, 1.8 mM $MgCl_2$, 5 mM $K_3Fe(CN)_6$, 5 mM $K_4Fe(CN)_6 \cdot 3H_2O$, and 1 mg/ml X-gal in dimethylformamide. Plates were incubated overnight at 37 °C and then photographed with a light microscope.

Supporting Information Available: Structural properties, synthetic procedures, and analytical data (NMR, HRMS, and combustion) for new compounds.This material is available free of charge via the Internet at http://pubs.acs.org.

References

(1) Wells, R. D. Non-B DNA conformations, mutagenesis and disease. *Trends Biochem. Sci.* **2007**, *32*, 271–278.

(2) Davis, J. T. G-quartets 40 years later: from 5′-GMP to molecular biology and supramolecular chemistry. *Angew. Chem., Int. Ed.* **2000**, *43*, 668–698.

(3) Burge, S.; Parkinson, G. N.; Hazel, P.; Todd, A. K.; Neidle, S. Quadruplex DNA: sequence, topology and structure. *Nucleic Acids Res.* **2006**, *34*, 5402–5415.

(4) Bailey, S. M.; Murnane, J. P. Telomeres, chromosome instability and cancer. *Nucleic Acids Res.* **2006**, *34*, 2408–2417.

(5) Gilson, E.; Londono-Vallejo, A. Telomere Length Profiles in Humans: All Ends are Not Equal. *Cell Cycle* **2007**, *6*, 2486–2494.

(6) Blackburn, E. H. Switching and signaling at the telomere. *Cell* **2001**, *106*, 61–73.

(7) Shay, J. W.; Bacchetti, S. A survey of telomerase activity in human cancer. *Eur. J. Cancer* **1997**, *33*, 787–791.

(8) Kelland, L. Targeting the limitless replicative potential of cancer: the telomerase/telomere pathway. *Clin. Cancer Res.* **2007**, *13*, 4960–4963.

(9) (a) Oganesian, L.; Bryan, T. M. Physiological relevance of telomeric G-quadruplex formation: a potential drug target. *Bioessays* **2007**, *29*, 155–165. (b) Pagano, B.; Giancola, C. Energetics of quadruplex-drug recognition in anticancer therapy. *Curr. Cancer Drug Targets* **2007**, *7*, 520–540. (c) Gunaratnam, M.; Greciano, O.; Martins, C.; Reszka, A. P.; Schultes, C. M.; Morjani, H.; Riou, J. F.; Neidle, S. Mechanism of acridine-based telomerase inhibition and telomere shortening. *Biochem. Pharmacol.* **2007**, *74*, 679–689. (d) Riou, J. F. G-quadruplex interacting agents targeting the telomeric G-overhang are more than simple telomerase inhibitors. *Curr. Med. Chem. Anticancer Agents* **2004**, *4*, 439–443.

(10) See for example: (a) Sun, D.; Thompson, B.; Cathers, B. E.; Salazar, M.; Kerwin, S. M.; Trent, J. O.; Jenkins, T. C.; Neidle, S.; Hurley, L. H. Inhibition of human telomerase by a G-quadruplex-interactive compound. *J. Med. Chem.* **1997**, *40*, 2113–2116. (b) Kim, M. Y.; Vankayalapati, H.; Shin-Ya, K.; Wierzba, K.; Hurley, L. H. Telomestatin, a potent telomerase inhibitor that interacts quite specifically with the human telomeric intramolecular G-quadruplex. *J. Am. Chem. Soc.* **2002**, *124*, 2098–2099. (c) Leonetti, C.; Amodei, S.; D'Angelo, C.; Rizzo, A.; Benassi, B.; Antonelli, A.; Elli, R.; Stevens, M. F. G.; D'Incalci, M.; Zupi, G.; Biroccio, A. Biological activity of the G-quadruplex ligand RHPS4 (3,11-difluoro-6,8,13-trimethyl-8*H*-quino[4,3,2-*kl*]acridinium methosulfate) is associated with telomere capping alteration. *Mol. Pharm.* **2004**, *66*, 1138–1146. (d) Pennarun, G.; Granotier, C.; Gauthier, L. R.; Gomez, D.; Hoffschir, F.; Mandine, E.; Riou, J.-F.; Mergny, J.-L.; Maillet, P.; Boussin, F. D. Apoptosis related to telomere instability and cell cycle alterations in human glioma cells treated by new highly selective G-quadruplex ligands. *Oncogene* **2005**, *24*, 2917–2928. (e) Monchaud, D.; Teulade-Fichou, M.-P. A hitchhiker's guide to G-quadruplex ligands. *Org. Biomol. Chem.* **2008**, *6*, 627−636.

(11) Lown, J. W.; Morgan, A. R.; Yen, S. F.; Wang, Y. H.; Wilson, W. D. Characteristics of the binding of the anticancer agents mitoxantrone and ametantrone and related structures to deoxyribonucleic acids. *Biochemistry* **1985**, *24*, 4028–4035.

(12) (a) Collier, D. A.; Neidle, S. Synthesis, molecular modeling, DNA binding, and antitumor properties of some substituted amidoanthraquinones. *J. Med. Chem.* **1988**, *31*, 847–857. (b) Fox, K. R.; Polucci, P.; Jenkins, T. C.; Neidle, S. A molecular anchor for stabilizing triple-helical DNA. *Proc. Natl. Acad. Sci. U.S.A.* **1995**, *92*, 7887–7891. (c) Perry, P. J.; Gowan, S. M.; Reszka, A. P.; Polucci, P.; Jenkins, T. C.; Kelland, L. R.; Neidle, S. 1,4- and 2,6-disubstituted amidoanthracene-9,10-dione derivatives as inhibitors of human telomerase. *J. Med. Chem.* **1998**, *41*, 3253–3260. (d) Perry, P. J.; Reszka, A. P.; Wood, A. A.; Read, M. A.; Gowan, S. M.; Dosanjh, H. S.; Trent, J. O.; Jenkins, T. C.; Kelland, L. R.; Neidle, S. Human telomerase inhibition by regioisomeric disubstituted amidoanthracene-9,10-diones. *J. Med. Chem.* **1998**, *41*, 4873–4884. (e) Agbandje, M.; Jenkins, T. C.; McKenna, R.; Reszka, A. P.; Neidle, S. Anthracene-9,10-diones as potential anticancer agents. Synthesis, DNA-binding, and biological studies on a series of 2,6-disubstituted derivatives. *J. Med. Chem.* **1992**, *35*, 1418–1429.

(13) Zagotto, G.; Sissi, C.; Moro, S:.; Ben, D. D.; Parkinson, G. N.; Fox, K. R.; Neidle, S.; Palumbo, M. Amide bond direction modulates G-quadruplex recognition and telomerase inhibition by 2,6 and 2,7 bis-substituted anthracenedione derivatives. *Bioorg. Med. Chem.* **2008**, *16*, 354–361.

(14) (a) Risitano, A.; Fox, K. R. Stability of intramolecular DNA quadruplexes: comparison with DNA duplexes. *Biochemistry.* **2003**, *42*, 6507–6513. (b) Darby, R. A.; Sollogoub, M.; McKeen, C.; Brown, L.; Risitano, A.; Brown, N.; Barton, C.; Brown, T.; Fox, K. R. High throughput measurement of duplex, triplex and quadruplex melting curves using molecular beacons and a LightCycler. *Nucleic Acids Res.* **2002**, *30*, e39. (c) De Cian, A.; Guittat, L.; Kaiser, M.; Sacca, B.; Amrane, S.; Bourdoncle, A.; Alberti, P.; Teulade-Fichou, M. P.; Lacroix, L.; Mergny, J. L. Fluorescence-based melting assays for studying quadruplex ligands. *Methods* **2007**, *42*, 183–195.

(15) Kim, N. W.; Wu, F. Advances in quantification and characterization of telomerase activity by the telomeric repeat amplification protocol (TRAP). *Nucleic Acids Res.* **1997**, *25*, 2595–2597.

(16) De Cian, A.; Cristofari, G.; Reichenbach, P.; De Lemos, E.; Monchaud, D.; Teulade-Fichou, M.-P.; Shin-Ya, K.; Lacroix, L.; Lingner, J.; Mergny, J.-L. Re-evaluation of telomerase inhibition by quadruplex ligands and their mechanisms of action. *Proc. Natl. Acad. Sci. U.S.A.* **2007**, *104*, 17347–17352.

(17) Masutomi, K.; Yu, E. Y.; Khurts, S.; Ben-Porath, I.; Currier, J. L.; Metz, G. B.; Brooks, M. W.; Kaneko, S.; Murakami, S.; DeCaprio, J. A.; Weinberg, R. A.; Stewart, S. A.; Hahn, W. C. Telomerase Maintains Telomere Structure in Normal Human Cells. *Cell.* **2003**, *114*, 241–253.

(18) Crothers, D. M. Statistical thermodynamics of nucleic acid melting transitions with coupled binding equilibria. *Biopolymers* **1971**, *10*, 2147–2160.

(19) Gatto, B.; Zagotto, G.; Sissi, C.; Cera, C.; Uriarte, E.; Palù, G.; Capranico, G.; Palumbo, M. Peptidyl anthraquinones as potential antineoplastic drugs: synthesis, DNA binding, redox cycling, and biological activity. *J. Med. Chem.* **1996**, *39*, 3114–3122.

(20) Dimri, G. P.; Lee, X.; Basile, G.; Acosta, M.; Scott, G.; Roskelley, C.; Medrano, E. E.; Linskens, M.; Rubelj, I.; Pereira -Smith, O.; Peacocke, M.; Campisi, J. A Biomarker that Identifies Senescent Human Cells in Culture and in Aging Skin in vivo. *Proc. Natl. Acad. Sci. U.S.A.* **1995**, *92*, 9363–9367.

(21) Huang, F.-C.; Chang, C.-C.; Lou, P.-J.; Kuo, I.; Chien, C.-W.; Chen, C.-T.; Shieh, F.-Y.; Chang, T.; Lin, J.-J. G-Quadruplex stabilizer 3,6-bis(1-methyl-4-vinyl pyridinium)carbazole diiodide induces accelerated senescence and inhibits tumorigenic properties in cancer cells. *Mol. Cancer. Res.* **2008**, *6*, OF1–OF10.

(22) Todd, A. K.; Johnston, M.; Neidle, S. Highly prevalent putative quadruplex sequence motifs in human DNA. *Nucleic Acids Res.* **2005**, *33*, 2901–2907.

JM800160V